

## Multi-scale Approach from Atomistic to Macro for Simulation of the Elastic Properties of Cement Paste

Tavakoli, Davoud; Gao, Peng; Tarighat, Amir ; Ye, Guang

**DOI**

[10.1007/s40996-019-00288-6](https://doi.org/10.1007/s40996-019-00288-6)

**Publication date**

2020

**Document Version**

Accepted author manuscript

**Published in**

Iranian Journal of Science and Technology - Transactions of Civil Engineering

**Citation (APA)**

Tavakoli, D., Gao, P., Tarighat, A., & Ye, G. (2020). Multi-scale Approach from Atomistic to Macro for Simulation of the Elastic Properties of Cement Paste. *Iranian Journal of Science and Technology - Transactions of Civil Engineering*, 44(3), 861-873. <https://doi.org/10.1007/s40996-019-00288-6>

**Important note**

To cite this publication, please use the final published version (if applicable).  
Please check the document version above.

**Copyright**

Other than for strictly personal use, it is not permitted to download, forward or distribute the text or part of it, without the consent of the author(s) and/or copyright holder(s), unless the work is under an open content license such as Creative Commons.

**Takedown policy**

Please contact us and provide details if you believe this document breaches copyrights.  
We will remove access to the work immediately and investigate your claim.

[Click here to view linked References](#)

1  
2  
3  
4  
5 **Multi-scale approach from atomistic to macro for**  
6 **simulation of the elastic properties of cement paste**  
7

8  
9 **Davoud Tavakoli <sup>a,b</sup>, Peng Gao <sup>a,c</sup>, Amir Tarighat <sup>b,\*</sup>, Guang Ye <sup>a</sup>**  
10

11  
12  
13 <sup>a</sup> Section Materials and Environment, Faculty of Civil Engineering and  
14 Geosciences, Delft University of Technology, Delft, The Netherlands  
15

16  
17 <sup>b</sup> Department of Civil Engineering, Shahid Rajaei Teacher Training  
18 University, Tehran, Iran  
19

20  
21 <sup>c</sup> School of Materials Science and Engineering, South China  
22 University of Technology, Guangzhou 510640, China  
23

24  
25 \* Corresponding author: D.Tavakoli, Shahid Rajaei Teacher training  
26 university, Lavizan, Shabanloo St., Tehran, Iran, Tel. 22970060, Fax.  
27 22970033. Email: D. Tavakoli: d.tavakoli@sru.ac.ir  
28  
29  
30  
31  
32  
33  
34  
35  
36  
37  
38  
39  
40  
41  
42  
43  
44  
45  
46  
47  
48  
49  
50  
51  
52  
53  
54  
55  
56  
57  
58  
59  
60  
61  
62  
63  
64  
65

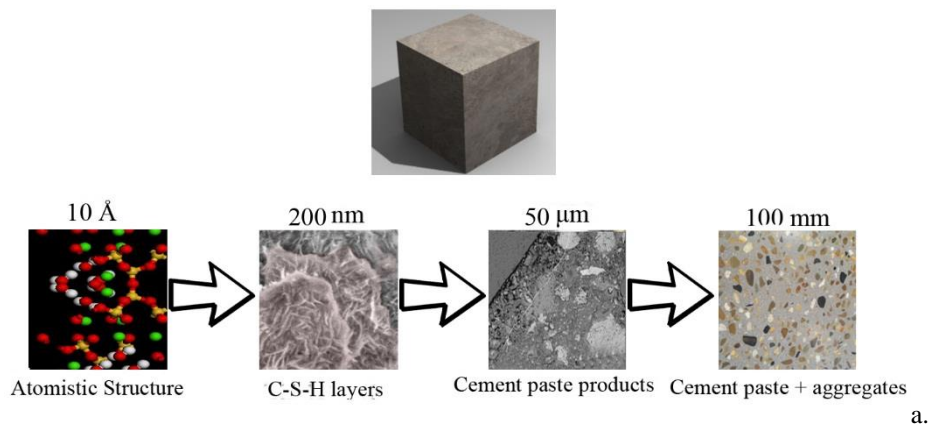
1  
2  
3  
4  
5 **Abstract**  
6

7 In this study first of all, the atomistic structure of cement hydration products are estimated  
8 via molecular dynamics method and their elastic properties are extracted. Then, cement  
9 hydration simulation is done by HYMOSTRUC3D model and the obtained results from  
10 both molecular dynamics and HYMOSTRUC3D methods are used for simulation in macro  
11 scales through analytic and lattice methods. Finally, elastic properties of cement paste are  
12 estimated with two mentioned method and compared with each other and also literature.  
13 The study, in fact, aims to investigate an appropriate multi-scale simulation model to  
14 examine cement paste elastic properties.  
15

16 **Keywords:** Molecular Dynamics; Hymostruc3D; cement past; lattice model; elastic  
17 properties.  
18

19  
20 **1. Introduction**  
21

22 Concrete is a complicated multi-scale material. If we categorize the concrete in some levels  
23 (Fig. 1): level zero includes atomistic solid material for C-S-H (Calcium silicate hydrate);  
24 level one is C-S-H layers along with gel pores; level two is cement paste incorporating a  
25 combination of C-S-H capillary pores and other hydration products including Portlandite  
26 (Calcium hydroxide (CH)), Ettringite, and un-hydrated cement grains; and level three  
27 entails cement paste in combination with aggregate. Cement paste consists of three main  
28 component (Taylor 1997). The most important of which is C-S-H that comprises 60% by  
29 volume in a fully hydrated cement paste. C-S-H exists in two forms of low density (LD)  
30 and high density (HD) in hydrated cement paste (Constantinides & Ulm 2007). These two  
31 differ in terms of amount of porosity in the component. The second material is Portlandite  
32 (CH) that plays an important role after C-S-H in cement paste. The other component in  
33 cement paste is un-hydrated cement grains that has not reacted with water.  
34  
35  
36  
37  
38  
39



54 Fig. 1. Multi-scale structure of concrete

1  
2  
3  
4  
5  
6  
7 Examining the nano-structure of materials is of great importance in examining their  
8 properties as knowing about nano-structure might lead to profound improvement in  
9 properties of materials. In addition, if a suitable modeling is done on the atomistic structure  
10 of materials, it will be possible to predict properties in macro-level via analytic, statistics  
11 methods or multi-scale and as a result of this, it becomes possible to make changes in the  
12 nano-structure and compare its results in macro-scale. One of the best used atomistic  
13 simulation methods is the molecular dynamics method (MD). The results of different  
14 studies have indicated that molecular dynamics is a powerful method in both simulation of  
15 different materials and prediction of mechanical properties and it has recently been used in  
16 most of studies (Tarighat et al. 2016). Given its powerful performance, the present study  
17 used the same method to examine the nano-structure of products in cement paste.  
18

19 Cement paste simulation at nano-scale is a new topic and atomistic investigation of  
20 cement paste has recently been done. Manzano et al. (2007) managed to reach the  
21 mechanical properties of cement paste by minimization of C-S-H structure energy. They  
22 simulated different compositions of C-S-H and their mechanical properties were obtained.  
23 Subramani et al. (2009) examined the mechanical properties of C-S-H gel via molecular  
24 dynamics methods by modeling some of tobermorite and foshagite. Subramani also looked  
25 into the attack of magnesium ions to cement paste and calculated the potential energy of  
26 crystal structure of C-S-H equivalent. Shahsavari et al. (2011) also examined the possibility  
27 of using different force fields and effects of changes in force fields on simulation results.  
28 The mechanical properties of Portlandite was examined in a study (Hajilar & Shafei 2016).  
29 Additionally, researchers dealt with the mechanical properties of calcium silicate hydrate  
30 (Dharmawardhana et al. 2016). Hajilar and Shafei (2015) investigated the use of molecular  
31 dynamics methods in simulation of cement hydration products. Zehtab and Tarighat (2016)  
32 investigated Diffusion of chloride ions in C-S-H by molecular dynamics method. Tavakoli  
33 et al. (2017) studied the effect of water on C-S-H properties. Finally, Tavakoli and Tarighat  
34 (2016) examined the elastic properties of cement phases.  
35

36 Moreover, Multi scale approach for concrete were done in some study (Liu & Wang  
37 2015, Wu & Xiao 2017, Sun et al. 2015).  
38

39 The present study touches on the examination of elastic properties of CH, C-S-H and  
40 un-hydrated cement by using molecular dynamics method. Upscaling the elastic properties  
41 of cement paste from atomistic scale to micro scale by using HYMOSTRUC3D model,  
42 lattice model as well as analytic methods were studied.  
43

44 HYMOSTRUC3D is a numerical model for cement paste simulation (van Breugel  
45 1995). Several studies have been carried out to simulate the properties of cement-based  
46 materials using this code, including cement hydration (van Breugel 1991, Gao et al. 2013,  
47 Ye et al. 2003), autogenous shrinkage of cement paste (Koenders 1997), and pore structure  
48 of cement paste (Ye 2003) The present study applies HYMOSTRUC3D to simulate the  
49 microstructure of cement paste.  
50

51 Furthermore, to reach the macro structure properties, lattice finite element analysis  
52 method was used to simulate the elastic properties of cement paste. Lattice finite element  
53 analysis method (Byung-Wan et al. 2005) has been used to model the mechanical  
54  
55  
56  
57  
58  
59  
60  
61  
62  
63  
64  
65

1  
2  
3  
4  
5 properties of materials for many years. In recent years, a GLAK (Generalized Lattice  
6 Analysis Kernel) program that is based on the lattice finite element analysis principle have  
7 been developed by Qian et al. (2010) to simulate the tensile strength of cement paste and  
8 concrete. This program has also been used to simulate the fracture behavior of cement paste  
9 (Luković et al. 2015), the cracking of concrete due to reinforcement corrosion (Šavija et  
10 al. 2013), and for multi-scale modeling (Zhang et al. 2016).

11  
12 Lastly, in this study, the mechanical properties of cement paste were simulated by both  
13 multi-scale modeling approach and analytic methods. The resulted findings were compared  
14 with the results of experimental studies.  
15

## 16 **2. Methods**

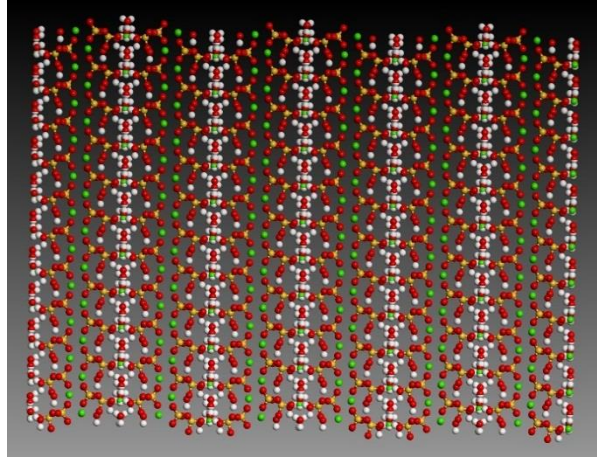
### 17 **2.1. Molecular dynamics**

18  
19  
20 Molecular dynamics is a powerful method to examine the chemical and physical properties  
21 of different materials (Al-Matar et al. 2015). This method is typically used for better  
22 understanding of physical and chemical interactions among atoms and obtaining the main  
23 properties in atomistic scale. In this method, the trajectories of molecules and atoms are  
24 specified by numerical calculation of movement equations for a system of particles that are  
25 interacting with each other. Potential energy and the inter-particles force are also  
26 determined by inter-atom potentials or force fields. The physical characters are then  
27 determined in terms of movement paths by thermodynamic and statistical physics rules  
28 (Tavakoli & Tarighat 2016). One of the most important parts of molecular dynamics is  
29 choosing a suitable force field for simulation. Force fields to calculate the potential energy  
30 of particles system use a combination of different parameters. In line with the literature,  
31 the present study uses force fields of COMPASS, COMPASS II, CLAY FF, and  
32 INTERFACE. According to the technical literature, the COMPASS force field is suitable  
33 for simulation of cement based materials (Dharmawardhana et al. 2016, Hajilar & Shafei  
34 2015).  
35

36  
37  
38 COMPASS II is, in fact, the modified version of COMPASS and seems to be suitable for  
39 cement based materials (Tavakoli & Tarighat 2016). Additionally, choosing a suitable  
40 force field for un-hydrated cement phases has been examined in a study in which  
41 INTERFACE and CLAY FF in addition to COMPASS group have been selected as suitable  
42 force fields (Tavakoli & Tarighat 2016).  
43

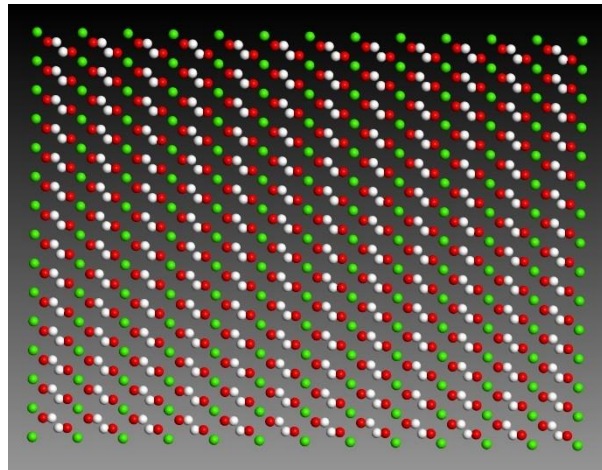
44  
45 For molecular dynamics simulation, it is necessary to first determine and create  
46 atomistic structure of materials. Due to the fact that the exact atomistic structure of C-S-H  
47 has not yet been known, several crystal simulation structures have been offered. Among  
48 these, Tobermorite 11Å and 14Å are remarkably similar to C-S-H where Tobermorite 14Å  
49 is more hydrated than Tobermorite 11Å (Merlino et al. 1999, Manzano 2014). Also,  
50 simulation results have shown that Tobermorite 14Å has more similar elastic properties to  
51 C-S-H than Tobermorite 11Å (Manzano 2014). As a result, the present study uses  
52 Tobermorite 14Å as the primary structure to simulate C-S-H. The chemical composition  
53 of tobermorite 14Å is  $\text{Ca}_5\text{Si}_6\text{O}_{16}(\text{OH})_{2.7}\text{H}_2\text{O}$ . Tobermorite 14Å has a monoclinic unit  
54

1  
2  
3  
4  
5  
6 cell with space group B11b and its Ca/Si ratio is 0.83 (Bonaccorsi 2005). The crystalline  
7 structures of tobermorite 14Å is shown in Fig. 2 and lattice parameters are shown in Table  
8 1.  
9



10  
11  
12  
13  
14  
15  
16  
17  
18  
19  
20  
21  
22  
23  
24  
25  
26 Fig. 2. Crystalline structure of Tobermorite 14 Å (white spheres: hydrogen ions; red  
27 spheres: Oxygen atoms; yellow spheres: silicon atoms; green spheres: calcium ions)  
28

29  
30 Calcium hydroxide (CH) constitutes about 20% by volume in a fully of hydrated  
31 cement paste. The crystal structure of CH was determined exactly. The chemical  
32 composition of CH is  $\text{Ca}(\text{OH})_2$  and has a trigonal unit cell with space group  $\text{Pm}\bar{3}1$   
33 (Halstead & moore 1957). The crystalline structure of CH is shown in Fig.3 and lattice  
34 parameters are illustrated in Table 1.  
35



36  
37  
38  
39  
40  
41  
42  
43  
44  
45  
46  
47  
48  
49  
50  
51 Fig. 3. Crystalline structure of Calcium hydroxide (white spheres: hydrogen ions; red  
52 spheres: Oxygen atoms; green spheres: calcium ions)  
53  
54  
55  
56  
57  
58  
59  
60  
61  
62  
63  
64  
65

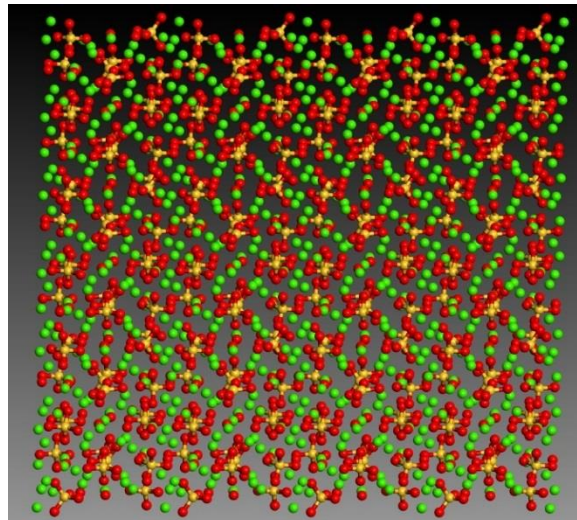
1  
2  
3  
4  
5 For unhydrated cement (U-Cement) grain, it is first necessary to simulate the cement  
6 clinker phases and then calculate its elastic properties. There are four main phases in  
7 cement clinker including C3S, C2S, C3A, and C4AF. The most important phase is C3S  
8 (Alite), is a name for tricalcium silicate ( $\text{Ca}_3\text{SiO}_5$ ), constitutes almost 50% to 70% by  
9 weight of cement clinker and plays an important role in cement properties (Bournazel et  
10 al. 1998, Biernacki & Gottapu 2015). The crystalline structure of C3S is triclinic with P1  
11 space group (Fig. 4). The lattice parameters of the alite are shown in Table 1. The second  
12 important phase is C2S (Belite), dicalcium silicate ( $\text{Ca}_2\text{SiO}_4$ ), that comprises almost 15%  
13 to 30% by weight of cement clinker. C2S also has various polymorphs and it is normally  
14 formed as the  $\beta$  polymorph. The unit cell of  $\beta$ -C2S is monoclinic with P21/c space group  
15 (Bournazel et al. 1998). The crystal structure of Belite is shown in Fig. 5 and lattice  
16 parameters are determined in Table 1.

17  
18  
19 Tricalcium aluminate (C3A) has the chemical composition of  $\text{Ca}_3\text{Al}_2\text{O}_6$ . It constitutes  
20 about 5%-10% by weight of cement clinker. C3A has a cubic unit cell with Pa3 space group  
21 (Mondal et al. 1975). The crystalline structure is illustrated in Fig. 6 and the lattice  
22 parameters are shown in Table 1.

23  
24 C4AF is the least important phase with chemical formula of  $\text{Ca}_2\text{AlFeO}_5$  and comprises  
25 about 5%-15% of cement clinker. The unit cell of C4AF is orthorhombic with Ibm2 space  
26 group (Kurdowski 2014). Fig.7 shows C4AF atomistic structure. The crystalline structure  
27 of C4AF are determined in Table 1.

28  
29 The minor phases of cement do not remarkably influence the physical properties of  
30 cement due to their slight component percent and are not considered in this study.

31 After preparing the crystal structure of materials, simulation process with minimization  
32 of energy is started. To simulate molecular dynamics, it is better to optimize the structure  
33 first and this is done by Smart method and after that, the simulation of molecular dynamics  
34 on the intended materials is done. Table 2 represents the details of simulation.



1  
2  
3  
4  
5  
6  
7  
8  
9  
10  
11  
12  
13  
14  
15  
16  
17  
18  
19  
20  
21  
22  
23  
24  
25  
26  
27  
28  
29  
30  
31  
32  
33  
34  
35  
36  
37  
38  
39  
40  
41  
42  
43  
44  
45  
46  
47  
48  
49  
50  
51  
52  
53  
54  
55  
56  
57  
58  
59  
60  
61  
62  
63  
64  
65

Fig. 4. Crystalline structure of alite (red spheres: Oxygen atoms; yellow spheres: silicon atoms; green spheres: calcium ions)

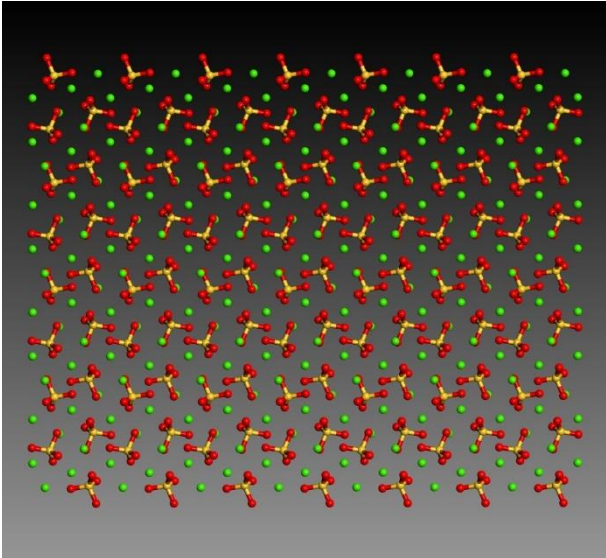


Fig. 5. Crystalline structure of Belite (red spheres: Oxygen atoms; yellow spheres: silicon atoms; green spheres: calcium ions)

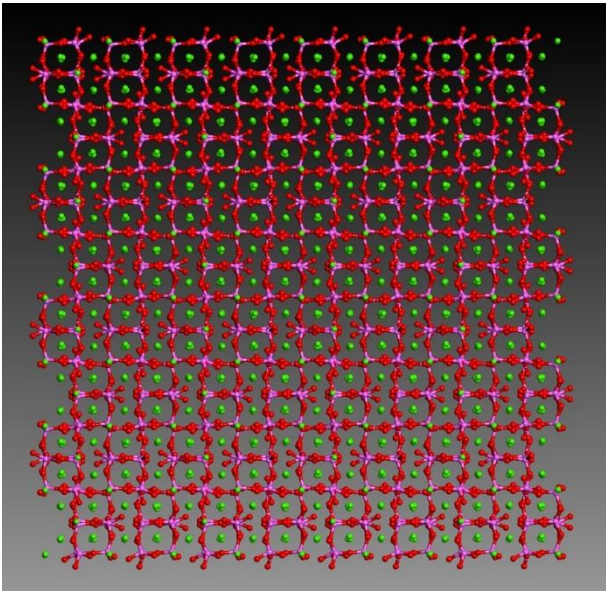


Fig. 6. Crystalline structure of Calcium aluminates (red: oxygen atoms; green: calcium ions; bluish pink: aluminum Ions)



1  
2  
3  
4  
5  
6  
7  
8  
9  
10  
11  
12  
13  
14  
15  
16  
17  
18  
19  
20  
21  
22  
23  
24  
25  
26  
27  
28  
29  
30  
31  
32  
33  
34  
35  
36  
37  
38  
39  
40  
41  
42  
43  
44  
45  
46  
47  
48  
49  
50  
51  
52  
53  
54  
55  
56  
57  
58  
59  
60  
61  
62  
63  
64  
65

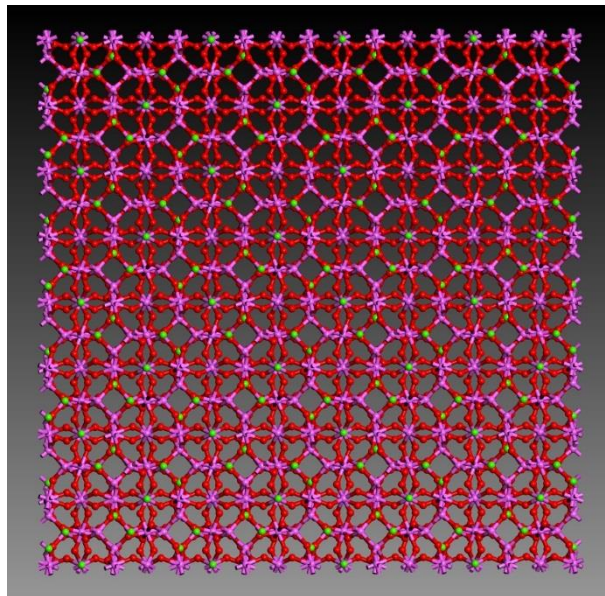


Fig. 7. Crystalline structure of calcium aluminate ferrite (red: oxygen atoms; green: calcium ions; blush pink: aluminum Ions)

Table 1. Crystallographic lattice parameters

Phases	$a$ (Å)	$b$ (Å)	$c$ (Å)	$\alpha$ (°)	$\beta$ (°)	$\gamma$ (°)
Tobermorite 14 Å <sup>a</sup>	6.73	7.42	27.98	90	90	123.25
Portlandite <sup>b</sup>	3.59	3.59	4.90	90	90	120
C3S <sup>c</sup>	11.63	14.17	13.64	104.9	94.6	90.1
C2S <sup>d</sup>	5.50	6.75	9.34	90	94.6	90
C3A <sup>e</sup>	15.26	15.26	15.26	90	90	90
C4AF <sup>f</sup>	5.58	14.6	5.37	90	90	90

a (Bonaccorsi et al. 2005), b (Mondal et al. 1975), c (Pollitt & Brown 1968), d (Pollitt & Brown 1959), e (Manzano et al. 2015), f (Tavakoli & Tarighat 2016)

Table 2. Simulation details

Parameters	Condition in this work
Force fields	COMPASS, COMPASS II, ClayFF, INTERFACE
Ensemble	NPT
Summation method	Ewald
Cut-off distance	12.5Å
Temperature	298 K (Room temperature)
Temperature control (MD)	Nosé thermostat
Pressure	0.0001 GPa (Air pressure)
Pressure control	Berendsen barostat
Dynamic time (MD)	500 ps to 1000 ps (based on the number of atoms)
Time step (MD)	1 fs
Boundary conditions	Three dimension periodic boundary condition
Maximum strain amplitude in each strain	0.003

For estimate the elastic properties of unhydrated cement grains, constant strain method was used. The elastic stiffness coefficients,  $C_{ijkl}$ , are estimated by Eq. 1 (Tavakoli & Tarighat 2016)

$$C_{ijkl} = \left. \frac{\partial \sigma_{ij}}{\partial \varepsilon_{kl}} \right|_{T, \varepsilon_{kl}} = \frac{1}{V_0} \left. \frac{\partial^2 A}{\partial \varepsilon_{ij} \partial \varepsilon_{kl}} \right|_{T, \varepsilon_{ij}, \varepsilon_{kl}} \quad (1)$$

Where,  $\sigma_{ij}$  is stress,  $\varepsilon_{kl}$  is strain, A is the Helmholtz free energy and  $V_0$  is the volume of the simulation cell.

By calculating two unconditional coefficients such as Shear modulus (G) and Bulk modulus (K), the elastic properties of unhydrated cement gran are estimated. K and G of the phases are calculated by Eq. 2 to Eq. 5 (Tavakoli & Tarighat 2016):

$$G_V = \frac{1}{15} [C_{11} + C_{22} + C_{33} + 3(C_{44} + C_{55} + C_{66}) - (C_{12} + C_{13} + C_{23})] \quad (2)$$

$$k_V = \frac{1}{9} [C_{11} + C_{33} + 2(C_{12} + C_{13} + C_{23})] \quad (3)$$

$$G_R = 15 [4(S_{11} + S_{22} + S_{33} - S_{12} - S_{13} - S_{23}) + 3(S_{44} + S_{55} + S_{66})]^{-1} \quad (4)$$

$$K_R = [S_{11} + S_{22} + S_{33} + 2(S_{12} + S_{13} + S_{23})]^{-1} \quad (5)$$

In these equations,  $S_{ij}$  shows the components of the elastic compliance matrix, R and V define the Reuss and the Voigt averages. Therefore, the average of Reuss and Voigt

values, which is known as Voigt-Reuss-Hill (VRH) approximation, can be estimated by Eq. 6 and Eq. 7 (Tavakoli & Tarighat 2016):

$$G_{VRH} = \frac{G_V + G_R}{2} \quad (6)$$

$$K_{VRH} = \frac{K_V + K_R}{2} \quad (7)$$

Finally, Elastic modulus (E) and Poisson's ratio ( $\nu$ ) are estimated by Eq. 8 and Eq. 9 (Tavakoli & Tarighat 2016):

$$E = \frac{9G}{3 + G/K} \quad (8)$$

$$\nu = \frac{3 - 2G/K}{6 + 2G/K} \quad (9)$$

In this study, Molecular dynamics simulations are done by Materials Studio package.

## 2.2. HYMOSTRUC3D model

When using multi-scale modelling approach at least two things should be clear: (1). Properties of each of the components. (2). The amount of each components. Properties of the components are determined by molecular dynamics method in this study. Besides, HYMOSTRUC3D code is used to determine the amount of each component. It is a numeric model to simulate cement paste. This model was developed in Delft University of Technology (van Breugel 1991). This code has been made to simulate cement hydration the micro-structure formation of hydrating cement paste. In this model, parameters such as cement particle size distribution, the chemical composition of used cement, water to cement ratio, and the curing temperature are considered. Cement particles in this model have been regarded as spheres and described using Rosin-Rammler distribution. In the initial step, cement particles are randomly distributed in a 3D cube (normally in the size of  $100 \times 100 \times 100 \mu\text{m}^3$ ). With hydration process, cement particles starts to partially dissolve and the C-S-H precipitate on the surface of unhydrated cement particles. This process is called expansion of cement particles. At the meantime, CH particles precipitate in the pore space. Given the hydration process, the expansion of cement particles leads to the interaction of particles and then, the microstructure structure of cement paste are obtained. Fig. 8 shows the interaction mechanism for cement particles in HYMOSTRUC model in a schematic way (van Breugel 1995). In hydration process, the state of cement particles might be categorized in three cases of un-hydrated cement, internal, and external products.

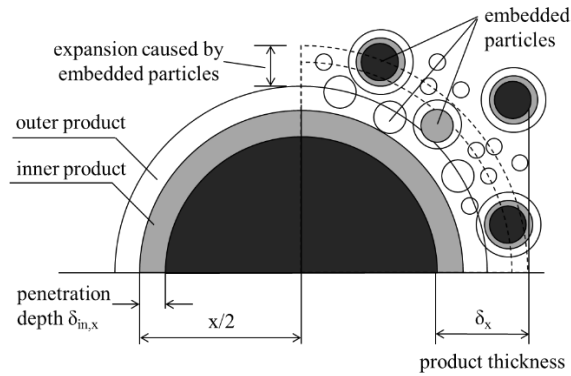


Fig. 8. Schematic diagram of the interaction mechanism for cement particles in HYMOSTRUC3D (van Breugel 1995)

To simulate cement hydration and microstructure by this model, the Type I cement is regarded as the input data. In a study that was conducted by XRD method and also Rietveld refinement technique, exact amounts of mineral phases composition in Type I cement was determined and the same amounts are used in the simulation so that the comparison would be more effective (Table 3) (Scrivener et al. 2004). It should, however, be pointed out that the HYMOSTRUC3D model simulates the hydration products in the form of high density C-S-H (HD-C-S-H), low density C-S-H (LD-C-S-H), CH, and un-hydrated cement do not consider the amounts of other hydration products owing to their trivial impact on physical properties of cement paste. Some hypotheses in the form of input for code are necessary for simulation that are shown in Table 3. Input data has been selected in a way that their results could be compared with those of experimental works.

After primary preparation of input file and primary features, a cube size with  $100 \mu\text{m}$  was chosen and the cement particles were put into it and then the simulation process in micro scale was done. In this simulation, the hydration process lasted for 500 days. However, given the importance of the 28 days curing age and many experimental data that exist for this age, the present study focused on 28 days.

Table 3. Input parameter for HYMOSTRUC3D

Parameter	Amount
C <sub>3</sub> S (%)	69.9
C <sub>2</sub> S (%)	8.30
C <sub>3</sub> A (%)	7.50
C <sub>4</sub> AF (%)	6.30
Gypsum (%)	2.90
Na <sub>2</sub> O (%)	0.19
K <sub>2</sub> O (%)	0.95
Water to cement ratio	0.4
Curing temperature (°C)	20
Maximum size of PC (μm)	50
Minimum size of PC (μm)	2
Cement Density (g/cm <sup>3</sup> )	3.15

### 2.3. Multi scale models

#### 2.3.1. Lattice model

Lattice model has been used to simulate the fracture process of cement-based materials for decades (Qian et al. 2010). Based on lattice model, Qian et al. (2010) have developed a program called GLAK (Generalized Lattice Analysis Kernel) package to simulate the fracture process of cement-based materials. By using GLAK program, the mechanical properties including tensile strength, elastic modulus, and etc., of cement-based materials can be predicted. The simulation process of GLAK program contains the construction of lattice mesh, and the imposing process of load on lattice mesh.

In this study the microstructure of cement paste simulated by HYMOSTRUC3D is firstly converted into lattice grid. As shown in Fig. 9, for each lattice grid, a sub cell is generated and a lattice node is randomly placed inside the sub cell. The Delaunay triangulation is used to connect the neighbor lattice nodes to produce lattice beams. An example of the construction of lattice mesh is shown in Fig. 10. As shown in Fig. 10b, in the simulation of tensile test, the bottom nodes are firstly fixed. Then, an incremental displacement is given at the top surface nodes to simulate the fracture process of lattice mesh. By the simulation of GLAK program, the reaction force at the top surface nodes can be obtained. Accordingly, stress-strain response of the cement paste can be simulated. Next, the stress-strain response curve is used to figure out the bulk elastic modulus of cement paste.

In the simulation, the input local mechanical properties of the lattice beams are assumed to be equal to the average of the local mechanical properties of the connected two nodes. The local mechanical properties of the connected two nodes are obtained from molecular dynamics simulation. In this way, the local mechanical properties of hydration products

simulated by molecular dynamics and microstructure of cement paste simulated by HYMOSTRUC3D are used to model the elastic modulus of cement paste in micro scale.

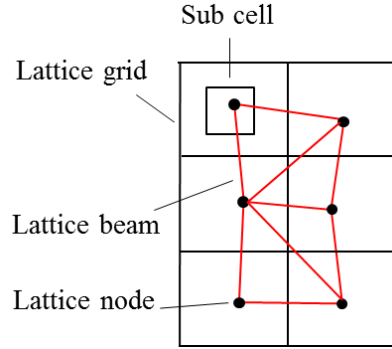


Fig. 9. Schematic diagram of the lattice mesh construction in this study

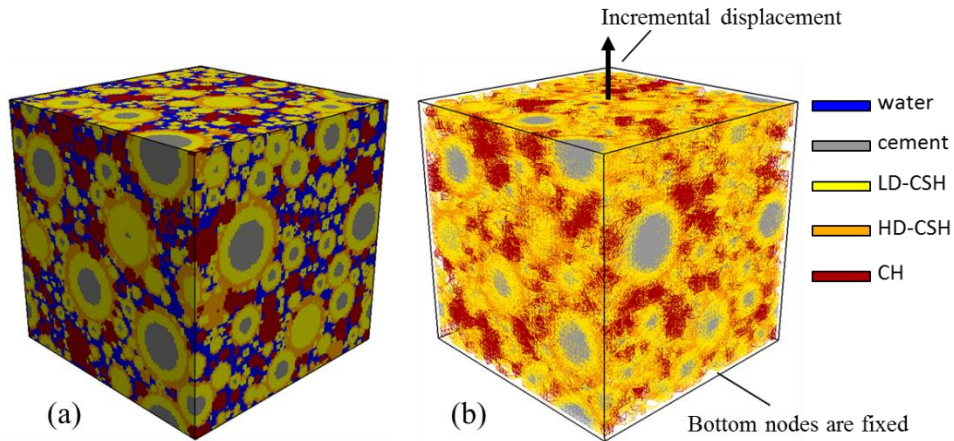


Fig. 10. An example of the construction of lattice mesh. (a) Microstructure of cement paste simulated by HYMOSTRUC3D (100×100×100 μm<sup>3</sup>); (b) the lattice mesh converted from microstructure, resolution = 8 μm<sup>3</sup>

### 2.3.2. Analytical method

As mentioned to predict the cement paste properties by micro mechanical models with analytical method, two parameters are needed: (1). Elastic modulus of each product (2). Volume fraction of each component. The former was calculated by molecular dynamics method and the latter can be obtained by HYMOSTRUC3D model.

The utilized micro mechanical model in this study is done in a set of stages. The basis of the model is based on the Jennings method (Tennis & Jennings 2000). The model is based on two precepts: (1). Un-hydrated cement is surrounded by HD-C-S-H, (2). CH tends

to grow between LD-C-S-H. To measure the Young modulus of cement paste, some steps should be done. In the first stage, the elastic modulus amounts are extracted by molecular dynamics method and volume fraction of each component are also obtained from HYMOSTRUC3D method. Given the point that Tobermorite 14Å is not exactly similar to C-S-H structure, and the real structure of C-S-H gel has internal pores and defects, Mori-Tanaka model (Mori & Tanaka 1973, Shokravi 2017) is employ to derive the elastic moduli of both HD-CSH and LD-CSH. According to this method, the effective shear (G) and bulk (K) moduli of the C-S-H gel can be estimated using the following equations:

$$G_{\text{CSH}} = G_{\text{solid}} \frac{(1 - \phi)(8G_{\text{solid}} + 9K_{\text{solid}})}{6\phi(2G_{\text{solid}} + K_{\text{solid}}) + 8G_{\text{solid}} + 9K_{\text{solid}}} \quad (10)$$

$$K_{\text{CSH}} = K_{\text{solid}} \frac{4G_{\text{solid}}(1 - \phi)}{3K_{\text{solid}}\phi + 4G_{\text{solid}}} \quad (11)$$

Where,  $\phi$  is the porosity of C-S-H gel. According to literature (Constantinides & Ulm 2007, Zhu et al. 2007) the porosities are 37% for LD- CSH and 24% for HD-CSH and by considering these amounts, elasticity modulus of C-S-H might be resulted.

To calculate the elastic modulus of unhydrated cement grain, different phases should be combined and the pores should be taken into consideration. Due to the close similarity of the elastic properties of these phases to each other, Voigt and Reuss model was used to reach a steadier elastic modulus. In Reuss model, different phases are put on each other in series and load is imposed on them (Monteiro 2006). However, in Voigt model, phases are inserted in parallel (Fig. 11) (Monteiro 2006). Generally, Voigt model shows a high upshot and Reuss model shows a low one and Hill model shows the average of them (Knudsen 1959). These models typically represent reasonable responses in cases where elastic properties are close to each other. This model is a simple model for composite and because different cement phases have very similar elastic properties and their arrangement structure is in the form of next to each other, it could be a suitable model for this material. Relations 12 and 13 show the Voigt and Reuss relations respectively (Knudsen 1959).

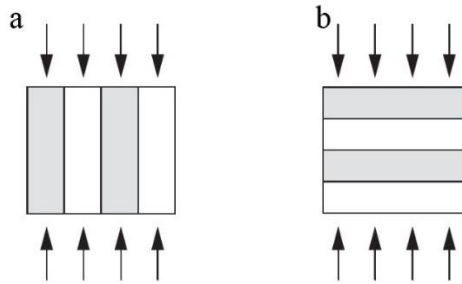


Fig. 11. Schematic of the (a) Voigt and the (b) Reuss methods (Monteiro 2006)

$$E = E_1 c_1 + E_2 c_2 \quad (12)$$

$$\frac{1}{E} = \frac{c_1}{E_1} + \frac{c_2}{E_2} \quad (13)$$

Where,  $c_i$  and  $E_i$  represent the volume fraction and Young's modulus of phase  $i$ ,  $i=1, 2$ . Unhydrated cement has a lot of porosity that is because of the arrangement of different phases next to each other or structure defects. Knudsen equation is used to introduce porosity in cement clinker structure (Eq. 14) (Knudsen 1959).

$$E = E_0 e^{-3.4\phi} \quad (14)$$

In these equations  $\phi$  is the porosity of clinker cement. To obtain the porosity amount of cement clinker, different methods might be used. Some studies have presented different results for porosity by analyzing the images from SEM and other methods. The reason for this difference is related to the type of cement and primary materials and components, kind of heating and cooling process and also manufacturing Process (Kurdowski 2014). Thus, it is not possible to offer an exact percentage for porosity. On the other hand, if analytic methods are used, packing density problem (Torquato & Stillinger 2007) might be used. In this method, by considering the point that particles in sphere or ellipse form, the empty space between them might be determined. The calculated porosity with this method is about 26% (Eq. 15). It should be noted that, this packing have the highest density amongst all possible lattice packing (Zohdi & Wriggers 2008).

$$\phi = 1 - \frac{\pi}{3\sqrt{2}} \approx 0.26 \quad (15)$$

This amount is good for the perfect spherical or elliptical grain and for irregular shape the porosity should be less than it. In the present study, in light of the obtained results and also the point that a wide range of amount are influential depending on the production method of cement and other factors, 20 % was considered for porosity of cement clinker that seems reasonable.

In the next stage, homogenization process is done. According to the stated principles, un-hydrated cement is put as inclusion in HD-C-S-H (composite 1) and CH as inclusion in LD-C-S-H (composite 2) and the homogenization process is done by Mori-Tanaka method. In this stage, the amount of inclusion and matrix components in each composite are determined by HYMOSTRUC3D method. In the next stage, composite 2 is put in the composite 1 matrix as inclusion and the homogenization process is done again. In the end, the determined porosity by HYMOSTRUC3D model for cement paste is inserted in the structure by pertinent relations (Eq. 10 and 11) and the final Young's modulus is calculated. The calculated porosity is equal to the sum of gel porosity and capillary porosity. To do the homogenization process, relations 16 and 17 were used to obtain G and K of each of the components and by using simple elasticity relations Young's modulus and poisson ratio of cement paste were calculated (Zohdi & Wriggers 2008). Fig. 12 shows the



homogenization process. Finally, the resulted findings were compared to those obtained from the experiments from lattice model based on multi-scale approach.

$$K = K_m + c(K_i - K_m) \frac{1}{1 + (1-c) \left[ \frac{K_i - K_m}{K_m + \frac{3}{4}K_m} \right]} \quad (16)$$

$$G = G_m + c(G_i - G_m) \frac{1}{1 + (1-c) \left[ \frac{G_i - G_m}{G_m + \frac{G_m(9K_m + 8G_m)}{6(K_m + 2K_m)}} \right]} \quad (17)$$

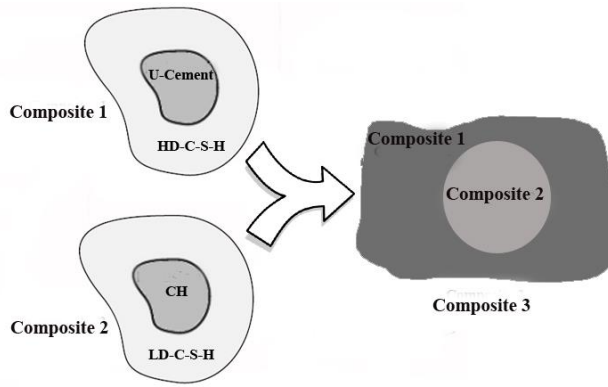


Fig. 12 Schematic of the homogenization

### 3. Results and Discussion

#### 3.1. Molecular dynamics

The calculated elastic properties of the phases of cement paste using molecular dynamics are shown in Table 4.

The results obtained from molecular dynamics for CH are considered as shown in the table. However, porosity in the structure should be taken into consideration for C-S-H. Additionally, homogenization process and consideration of porosity in the phases are essential for un-hydrated cement. For Tobermorite  $14\text{\AA}$ , the 24 % porosity was regarded for HD state and 37 % for LD state using Mori-Tanaka method. The obtained results for this material are presented in Table 5 after considering porosity and these values are remarkably in accordance with the results reported in the related literature (Constantinides & Ulm 2007, Jennings et al. 2007).

Furthermore, the elastic modulus has been calculated for un-hydrated cement after using Voigt and Reuss method and also considering 20% porosity. The results are shown in Table 6.

Table 4 Elastic properties of cement paste phases calculated by using MD

Crystal	K	G (GPa)	E (GPa)	$\nu$
Tobermorite 14Å	38.86	17.99	46.75	0.30
Portlandite	35.66	20.15	50.86	0.26
C <sub>3</sub> S	169.87	51.03	139.15	0.36
C <sub>2</sub> S	102.67	60.98	152.70	0.25
C <sub>3</sub> A	96.74	65.11	159.53	0.22
C <sub>4</sub> AF	163.25	79.59	205.39	0.29

Table 5 Young's modulus of C-S-H

C-S-H	LD-C-S-H	HD-C-S-H
E (GPa)	21.47	28.63

Table 6 Young's modulus of unhydrated cement

Model	Voigt model	Reuss model	Hill model	Hill model with porosity
E (GPa)	147.16	145.40	146.28	74.10

Displayed equations are to be centered on the page width. Standard English letters like  $x$  are to appear as  $x$  (italicized) in the text if they are used as mathematical symbols. Punctuation marks are used at the end of equations as if they appeared directly in the text.

### 3.2 HYMOSTRUC3D Model

The amounts of each of the above-mentioned phases were also obtained by HYMOSTRUC3D. The microstructural development of hydration cement paste is shown in Fig. 13.

The hydration process lasted up to 500 days and the volume fraction of each component has been estimated separately. Fig. 14 presents the growth trend of hydration products up to 500 days. As it is expected, the growth trend of hydration products (C-S-H and CH) is considerable in early ages and gradually decreases. Moreover, the curves related to porosity and un-hydrated cement start to drop as the increases of curing time. In fact, the primary cement is gradually turned into C-S-H and CH and the growth of them leads to filling of capillary pores in cement paste. The hydration production for 28 days curing days are show separately in Fig. 15.

1  
2  
3  
4  
5  
6  
7  
8  
9  
10  
11  
12  
13  
14  
15  
16  
17  
18  
19  
20  
21  
22  
23  
24  
25  
26  
27  
28  
29  
30  
31  
32  
33  
34  
35  
36  
37  
38  
39  
40  
41  
42  
43  
44  
45  
46  
47  
48  
49  
50  
51  
52  
53  
54  
55  
56  
57  
58  
59  
60  
61  
62  
63  
64  
65

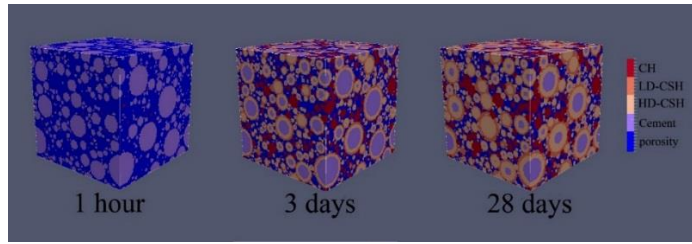


Fig. 13 Hydration process

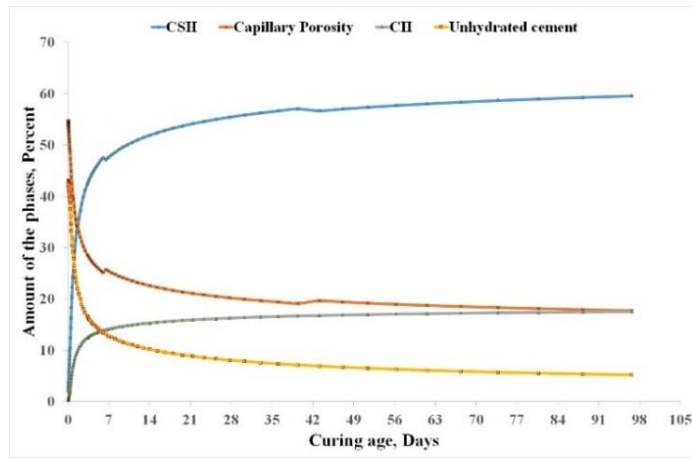


Fig. 14 Production of the hydrated cement products

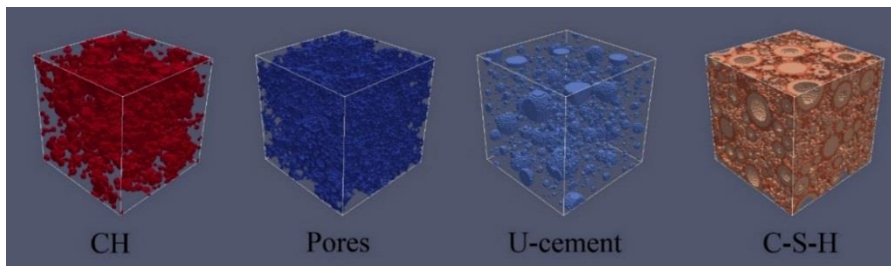


Fig. 15. Hydrated cement production in 28 days curing days

In general there are two types of porosity in cement: capillary porosity and gel porosity. Capillary porosity is developed between the hydration products and gel porosity is developed between the C-S-H layers. In the HYMOSTRUC3D simulation method, only the capillary porosity is regarded in the whole simulation and the interval between C-S-H layers is regarded as completely dense. The model calculates the gel porosity separately. The simulation cube is, in fact, a combination of solid materials and capillary porosity in unit volume and the gel porosity is then calculated and is not regarded as part of the simulation cell volume. Results of hydration products at 7, 28, and 90 days curing age are shown in Table 7.

Table 7. Phase volume fraction of the cement paste

products	7 days		28 days		90 days	
	Percent of total	Percent of solid phase	Percent of total	Percent of solid phase	Percent of total	Percent of solid phase
HD-C-S-H	31.43	42.14	36.18	45.35	38.88	47.36
LD-C-S-H	16.19	21.71	19.23	24.11	20.36	24.80
CH	14.13	18.94	16.29	20.42	17.46	21.27
Unhydrated cement	12.83	17.21	8.08	10.12	5.39	6.57
Total solid phase	74.58	100	79.78	100	82.09	100
Capillary porosity	25.42	-	20.22	-	17.91	-

Table 8 also presents the results related to gel porosity. In light of the point that the obtained results in different studies are mostly based on 28 days strength of cement paste, the present study also mainly dealt with the same cement paste. Thus, the results of 28 days are used for reaching a multi-scale modeling.

Table 8. Percentage of the gel porosity

Curing days	7 days	28 days	90 days
Percentage of the gel porosity	5.82	6.93	7.32

### 3.3 Multi-scale models

#### 3.3.1. Lattice model

The obtained elastic properties of phases from molecular dynamics (3.1) and microstructure from HYMOSTRUC3D model (3.2) were used as input for multi scale simulation of mechanical properties with lattice model (GLAK program). Based on lattice model, the stress-strain response for the cement pastes cured at different days are obtained. The simulation results are shown in Fig. 16. According to the stress-strain response, the Young's modulus of cement pastes are calculated. Table 9 lists the Young's modulus of cement pastes at the age of 7 days up to 90 days.

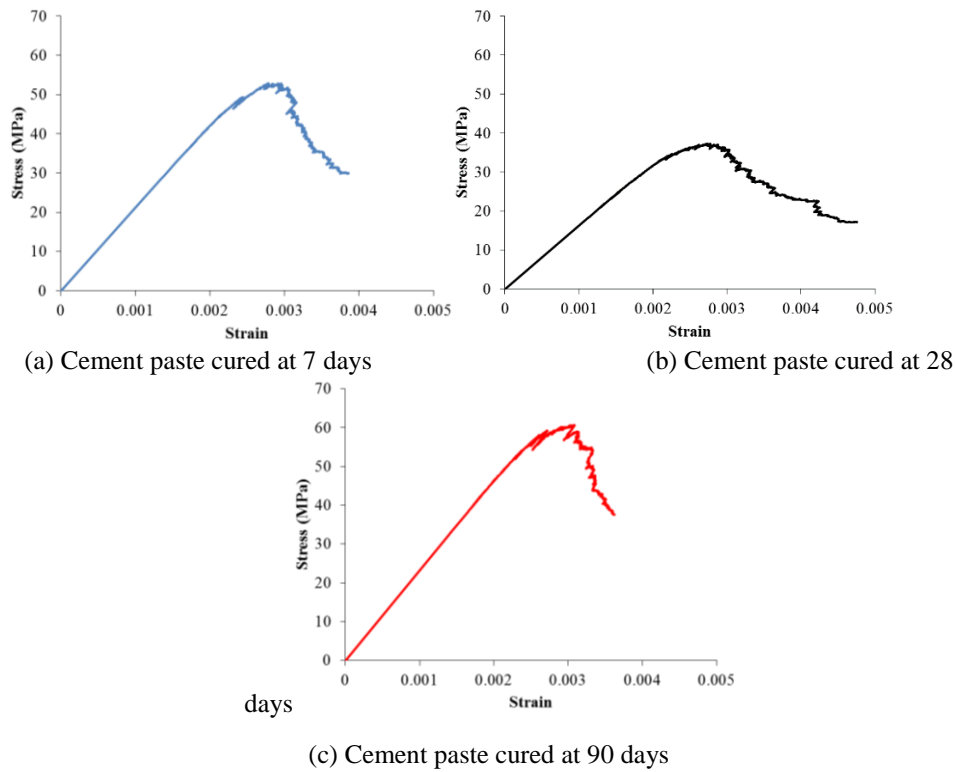


Fig. 16. Tensile test deformation of cement paste cured at 28 days (Delaunay triangle lattice mesh) - Note: The deformation is amplified for the convenience of visualization. Only the surface of lattice mesh at z and y axis are shown.

Table 9. Young's modulus of cement paste simulated by GLAK program

Yong's modulus (GPa)		
7 day	28 days	90 days
16.25	21.16	23.25

### 3.3.2. Analytical method

After calculating the elastic modulus and also the amounts of each of the components, the homogenization process was done based on the method presented in figure 11. The elastic modulus and poisson ratio for composite 3 was calculated by equations 5 and 6. These are for cement without porosity. As it was mentioned, one of the most important influential parameters on elastic properties is porosity. In this stage, it is necessary to take into consideration the paste porosity in the calculation of elastic properties. The calculated porosity is the sum of gel porosity and capillary porosity. The capillary and gel porosity estimated by HYMOSTRUC3D model are 20.22% and 6.93% for 28 days cement paste,

1  
2  
3  
4  
5  
6 respectively. Therefore, in the sum of these two numbers (27.15) is considered in  
7 calculations.

8 The final elastic properties were calculated and shown in Table 10.

9  
10  
11 Table 10. Elastic properties of composites

Parameters	Composite 1	Composite 2	Composite 3	Composite 3 with porosity (cement past)
K (GPa)	27.36	21,91	24.76	13.72
G (GPa)	18.67	14.75	16.03	9.24
E (GPa)	45.63	36.14	39.55	22.64
$\nu$	0.222	0.225	0.234	0.225

12  
13  
14  
15  
16  
17  
18  
19  
20  
21  
22 Young modulus that obtained from different method are shown in Table 11. Some  
23 previous conducted studies on the same issue are in line with the present study findings as  
24 discussed below.

25  
26  
27 Table 11. Elastic properties cement past

Method	Analytical method	Lattice model	References
E (GPa)	22.64	21.16	22.8± .05 <sup>a</sup> , 22-25 <sup>b</sup>

28  
29  
30  
31  
32 a Constantinides and Ulm (2004), b Haecker et al. (2005)

33  
34  
35  
36  
37  
38  
39  
40  
41  
42  
43  
44  
45  
46  
47  
48  
49  
50  
51  
52  
53  
54  
55  
56  
57  
58  
59  
60  
61  
62  
63  
64  
65  
The Young's modulus has been calculated to be 22.8± .05 GPa in a study by Constantinides and Ulm using nano-indentation method and the result obtained from the homogenization is exactly in accordance with this experimental result (Constantinides & Ulm, 2004). Furthermore, in another study, the elastic modulus for cement paste has been calculated to be between 22 and 25 GPa using finite elements method and this is also in the same range with the present study (Haecker 2005). The results that obtained from lattice model in part 3.3.1 also in accordance with analytical method results in part 3.3.2.

Given the obtained results, it might be stated that the offered pattern for multi-scale simulation is acceptable and it might be used to observe the effect of changes in nano structure of the products in the micro structure of cement paste.

#### 4. Conclusion

The current study dealt with the examination of possibility of multi-scale simulation for cement paste. To this goal, first, simulation in atomistic scale was done for different products by molecular dynamics method and their elasticity module was determined. Then, the process of cement hydration was simulated via HYMOSTRUC3D method and the amount of cement paste components were estimated. After that, the results of the molecular dynamics method and HYMOSTRUC3D model were used to calculate the Young's modules of the cement paste in micro scale with lattice model and also analytical model.

1  
2  
3  
4  
5 Finally, the obtained results from analytical method were compared with lattice model and  
6 with experimental results. The results revealed that multi-scale modeling with analytical  
7 method and lattice model was reported similar results and also literature results were  
8 confirmed them. It is concluded that the proposed multi-scale modeling approach could  
9 appropriately predict the elastic properties of cement paste.  
10

## 11 **References**

- 12  
13 Alder, B. J., & Wainwright, T. E. (1959). Studies in molecular dynamics. I. General  
14 method. *The Journal of Chemical Physics*, 31(2): 459-466.  
15  
16 Al-Matar, A. K., Tobgy, A. H., Suleiman, I. A., & Al-Faiad, M. A. (2015). Improving  
17 Monte-Carlo and molecular dynamics simulation outcomes using temperature-  
18 dependent interaction parameters: The case of pure LJ fluid. *International Journal of*  
19 *Computational Methods*, 12(02), 1550003.  
20  
21 Biernacki, J. J., & Gottapu, M. (2015). An advanced single-particle model for C3S  
22 hydration-validating the statistical independence of model parameters. *Computers and*  
23 *Concrete*, 15(6): 989-999.  
24  
25 Bonaccorsi, E., Merlino, S. & Kampf, A. R. (2005). The crystal structure of tobermorite  
26 14 Å (plombierite), a C–S–H phase. *Journal of the American Ceramic Society*. 88(3):  
27 505-512.  
28  
29 Bournazel, J.P., Malier, Y. & Moranville Regourd, M. (1998). Concrete: From Material to  
30 Structure Proceedings of the RILEM International Conference: Arles, France.  
31  
32 Constantinides, G. & Ulm, F. J. (2007). The nanogranular nature of C–S–H. *Journal of the*  
33 *Mechanics and Physics of Solids*, 55(1): 64-90.  
34  
35 Constantinides, G., & Ulm, F. J. (2004). The effect of two types of CSH on the elasticity  
36 of cement-based materials: Results from nanoindentation and micromechanical  
37 modeling. *Cement and concrete research*, 34(1): 67-80.  
38  
39 Dharmawardhana, C., Bakare, M., Misra, A., & Ching, W. Y. (2016). Nature of Interatomic  
40 Bonding in Controlling the Mechanical Properties of Calcium Silicate Hydrates.  
41 *Journal of the American Ceramic Society*, 99(6): 2120-2130.  
42  
43 Gao, Y., De Schutter, G., Ye, G., Yu, Z., Tan, Z., & Wu, K. (2013). A microscopic study  
44 on ternary blended cement based composites. *Construction and Building Materials*, 46:  
45 28-38.  
46  
47 Haecker, C. J., Garboczi, E. J., Bullard, J. W., Bohn, R. B., Sun, Z., Shah, S. P., & Voigt,  
48 T. (2005). Modeling the linear elastic properties of Portland cement paste. *Cement and*  
49 *Concrete Research*, 35(10): 1948-1960.  
50  
51 Hajilar, S. & Shafei, B. (2015). Nano-scale investigation of elastic properties of hydrated  
52 cement paste constituents using molecular dynamics simulations. *Computational*  
53 *Materials Science*, 101: 216-226.  
54  
55 Hajilar, S. & Shafei, B. (2016). Assessment of structural, thermal, and mechanical  
56 properties of portlandite through molecular dynamics simulations. *Journal of Solid*  
57 *State Chemistry*, 244: 164-174.  
58  
59  
60  
61  
62  
63  
64  
65

- 1  
2  
3  
4  
5  
6 Halstead, P.E. & moore, A.E. (1957). The thermal dissociation of calcium hydroxide. *J. Chem. Soc.*, 769: 3873–3875.  
7  
8 Janakiram Subramani, V., Murray, S., Panneer Selvam, R. & Hall, K. D. (2009). Atomic  
9 Structure of Calcium Silicate Hydrates Using Molecular Mechanics. *In Transportation*  
10 *Research Board 88th Annual Meeting* (No. 09-0200).  
11 Jennings, H. M., Thomas, J. J., Gevrenov, J. S., Constantinides, G., & Ulm, F. J. (2007). A  
12 multi-technique investigation of the nanoporosity of cement paste. *Cement and*  
13 *Concrete Research*, 37(3): 329-336.  
14 Jo, B. W., Tae, G. H., Schlangen, E., & Kim, C. H. (2005). Crack propagation simulation  
15 of concrete with the regular triangular lattice model. *Computers and Concrete*, 2(2):  
16 165-176.  
17 Knudsen, F.P. (1959). Dependence of mechanical strength of brittle polycrystalline  
18 specimens on porosity and grain size. *Journal of the American Ceramic Society*, 42:  
19 376-387  
20  
21 Koenders E.A.B. (1997). Simulation of volume changes in hardening cement-based  
22 materials. PhD Thesis, Delft, Delft University of Technology, The Netherlands.  
23 Kurdowski, W. (2014), Cement and concrete chemistry. Springer Science & Business.  
24 Liu, R., & Wang, L. (2015). Vibration of Cantilevered Double-Walled Carbon Nanotubes  
25 Predicted by Timoshenko Beam Model and Molecular Dynamics. *International Journal of*  
26 *Computational Methods*, 12(04), 1540017.  
27  
28 Luković, M., Schlangen, E., & Ye, G. (2015). Combined experimental and numerical study  
29 of fracture behaviour of cement paste at the microlevel. *Cement and Concrete*  
30 *Research*, 73: 123-135.  
31  
32 Manzano Moro, H. (2014). Atomistic simulation studies of the cement paste components.  
33 Servicio Editorial de la Universidad del País Vasco/Euskal Herriko Unibertsitatearen  
34 Argitalpen Zerbitzua.  
35  
36 Manzano, H., Dolado, J. S., Guerrero, A. & Ayuela, A. (2007). Mechanical properties of  
37 crystalline calcium-silicate-hydrates: comparison with cementitious C-S-H  
38 gels. *physica status solidi (a)*, 204(6): 1775-1780.  
39  
40 Manzano, H., Durgun, E., López-Arbeloa, I. & Grossman, J.C. (2015) *ACS Appl. Mater.*  
41 *Interfaces*, 7: 14726–14733  
42  
43 Merlino, S., Bonaccorsi, E., & Armbruster, T. (1999). Tobermorites: Their real structure  
44 and order-disorder (OD) character. *American Mineralogist*, 84: 1613-1621.  
45  
46 Mondal, P., & Jeffery, J. W. (1975). The crystal structure of tricalcium aluminate,  
47  $\text{Ca}_3\text{Al}_2\text{O}_6$ . *Acta Crystallographica Section B: Structural Crystallography and Crystal*  
48 *Chemistry*, 31(3): 689-697.  
49  
50 Monteiro, P. (2006), Concrete: Microstructure, Properties, and Materials. McGraw-Hill  
51 Publishing.  
52  
53 Mori, T., & Tanaka, K. (1973). Average stress in matrix and average elastic energy of  
54 materials with misfitting inclusions. *Acta metallurgica*, 21(5): 571-574.  
55  
56 Pollitt, H.W.W. & Brown, A.W. (1968), 5th ICCG Tokyo, vol. I, Tokyo, , 322  
57  
58 Qian, Z., Schlangen, E., Ye, G. & Van Breugel, K. (2010). Prediction of mechanical  
59 properties of cement paste at microscale. *Materiales de Construcción*, 60(297): 7-18.  
60  
61  
62  
63  
64  
65



- 1  
2  
3  
4  
5 Šavija, B., Luković, M., Pacheco, J., & Schlangen, E. (2013). Cracking of the concrete  
6 cover due to reinforcement corrosion: a two-dimensional lattice model study.  
7 *Construction and Building Materials*, 44: 626-638.
- 8  
9 Scrivener, K.L., Fullmann, T., Gallucci, E., Walenta, G. & Bermejo, E. (2004).  
10 Quantitative study of Portland cement hydration by X-ray diffraction/Rietveld analysis.  
11 *Cement and Concrete Research*, 34(9): 1541-1547
- 12  
13 Shahsavari, R., Pellenq, R. J. M. & Ulm, F. J. (2011), Empirical force fields for complex  
14 hydrated calcio-silicate layered materials, *Physical Chemistry Chemical*  
15 *Physics*, 13(3): 1002-1011.
- 16  
17 Shokravi, M. (2017). Vibration analysis of silica nanoparticles-reinforced concrete beams  
18 considering agglomeration effects. *Computers and Concrete*, 19(3): 333-338.
- 19  
20 Sun, B., Wang, X., & Li, Z. (2015). Meso-scale image-based modeling of reinforced  
21 concrete and adaptive multi-scale analyses on damage evolution in concrete structures.  
22 *Computational Materials Science*, 110, 39-53.
- 23  
24 Tarighat, A., Zehtab, B. & Tavakoli, D. (2016). An Introductory Review of Simulation  
25 Methods for the Structure of Cementitious Material Hydrates at Different Length  
26 Scales. *Pertanika Journal of Science & Technology (JST)*, 24(1): 27-39.
- 27  
28 Tavakoli, D. & Tarighat, A. (2016). Molecular dynamics study on the mechanical  
29 properties of Portland cement clinker phases. *Computational Materials Science*, 119:  
30 65-73.
- 31  
32 Tavakoli, D., Tarighat, A., & Beheshtian, J. (2017). Nanoscale investigation of the  
33 influence of water on the elastic properties of C-S-H gel by molecular simulation.  
34 *Proceedings of the Institution of Mechanical Engineers, Part L: Journal of Materials:*  
35 *Design and Applications*, 1464420717740926.
- 36  
37 Taylor, H.F. (2000), *Cement Chemistry*, second ed., Thomas Telford Publishing, London
- 38  
39 Tennis, P.D. & Jennings, H.M. (2000). A model for two types of calcium silicate hydrate in  
40 the microstructure of Portland cement pastes. *Cement and Concrete Research*, 30(6):  
41 855-863
- 42  
43 Torquato, S., & Stillinger, F. H. (2007). Toward the jamming threshold of sphere packings:  
44 Tunneled crystals. *Journal of Applied Physics*, 102(9): 093511.
- 45  
46 van Breugel, K. (1991). Simulation of hydration and formation of structure in hardening  
47 cement-based materials. PhD Thesis, Delft, Delft University of Technology, The  
48 Netherlands.
- 49  
50 van Breugel, K. (1995). Numerical Simulation of Hydration and Microstructural  
51 Development in Hardening Cement-Based Materials.(I) Theory. *Cement and Concrete*  
52 *Research*, 25(2): 319-331.
- 53  
54 Wu, Y., & Xiao, J. (2017). The Multiscale Spectral Stochastic Finite Element Method for  
55 Chloride Diffusion in Recycled Aggregate Concrete. *International Journal of*  
56 *Computational Methods*, 1750078.
- 57  
58 Ye, G. (2003). Experimental Study and Numerical Simulation of the Development of the  
59 microstructure and permeability of cementitious materials. PhD Thesis, Delft, Delft  
60 University of Technology, The Netherlands.
- 61  
62  
63  
64  
65

1  
2  
3  
4  
5  
6  
7  
8  
9  
10  
11  
12  
13  
14  
15  
16  
17  
18  
19  
20  
21  
22  
23  
24  
25  
26  
27  
28  
29  
30  
31  
32  
33  
34  
35  
36  
37  
38  
39  
40  
41  
42  
43  
44  
45  
46  
47  
48  
49  
50  
51  
52  
53  
54  
55  
56  
57  
58  
59  
60  
61  
62  
63  
64  
65

Ye, G., Van Breugel, K., & Fraaij, A. L. A. (2003). Experimental study and numerical simulation on the formation of microstructure in cementitious materials at early age. *Cement and Concrete Research*, 33(2): 233-239.

Zehtab, B., & Tarighat, A. (2016). Diffusion study for chloride ions and water molecules in CSH gel in nano-scale using molecular dynamics: Case study of tobermorite. *ADVANCES IN CONCRETE CONSTRUCTION*, 4(4): 305-317.

Zhang, H., Šavija, B., Chaves Figueiredo, S., Lukovic, M., & Schlangen, E. (2016). Microscale Testing and Modelling of Cement Paste as Basis for Multi-Scale Modelling. *Materials*, 9(11): 907.

Zhu, W., Hughes, J. J., Bicanic, N. & Pearce, C. J. (2007). Nanoindentation mapping of mechanical properties of cement paste and natural rocks. *Materials characterization*, 58(11): 1189-1198.

Zohdi, T. I., & Wriggers, P. (2008). An introduction to computational micromechanics. Springer Science & Business Media.